The object of the study is a six degrees-of-freedom motion system of the synergistic type of a flight simulator. The latter is the main technical means for training pilots and means of research and development of aircraft. The task of optimal utilization of its structural resources was solved, which provides an opportunity to improve the quality of motion cueing. The result is the developed method, which ensures optimal use of structural resources of motion systems of flight simulators. This is explained, first of all, by the use of the developed simplified operator for converting the movements of jacks into the movement of a motion system along individual degrees of freedom on the basis of quadratic approximation. Given this, it became possible to describe the coordinates of the centers of the axes of rotation of the motion system by cubic spline functions. Secondly, the solution of the task of estimating the structural resources of the motion system along linear degrees of freedom on the basis of the developed criterion was carried out by an effective modified method of the deformed polyhedron. This method combines the random search method in the first steps of the search and the gradient method in determining the global extremum. Thirdly, the problem of determining the dependence of the coordinates of the pitch and yaw axes along the pitch angle was stated and solved. Owing to the optimal utilization of the structural resources of motion systems, the coordinates of the axis of their rotation along pitch are as close as possible to the coordinate of the axis of the aircraft. Thus, the quality of motion cueing on the flight simulator is significantly increased and it is possible to use motion systems with shorter lengths of jacks, and therefore, to reduce the cost of their manufacture and operation

Keywords: jacks, motion system, structural resources, flight simulator, motion cueing

UDC 629.736.072.8; 681.3
DOI: 10.15587/1729-4061.2023.282129

OPTIMIZING THE UTILIZATION OF STRUCTURAL RESOURCES OF FLIGHT SIMULATOR MOTION SYSTEMS

Volodymyr Kabanyachyi
Doctor of Technical Sciences*
Serhii Hrytsan
Corresponding author
Postgraduate Student*
E-mail: serhii.v.hrytsan@gmail.com
*Department of Aircraft and Rocket Engineering
National Technical University of Ukraine «Igor Sikorsky Kyiv Polytechnic Institute»
Peremohy ave., 37, Kyiv, Ukraine, 03056

Received date 05.04.2023
Accepted date 08.06.2023
Published date 30.06.2023

How to Cite: *Kabanyachyi, V., Hrytsan, S. (2023). Optimizing the utilization of structural resources of flight simulator motion systems. Eastern-European Journal of Enterprise Technologies, 3 (1 (123)), 21–32. doi: https://doi.org/10.15587/1729-4061.2023.282129*

1. Introduction

Flight simulation can be defined as the creation in real time, under non-flight conditions, of the characteristics and operation of a specific aircraft. It also creates an environment that reacts with the necessary accuracy to detect the behavior of the pilot as if the flight is carried out in a real aircraft. Flight simulators are used mainly for two tasks: aircraft research and development, and crew training.

Full flight simulator (FFS) is a term used to denote a flight simulator of a higher technical level. FFS provides feedback to the crew about the movement through the six degrees-of-freedom motion system (DOF6), on which the simulator cabin is installed and the movement of which creates motion cues. DOF6 is one of the most important components of FFS (Fig. 1).

Scientific research on DOF6 is important because it expands knowledge about its capabilities. The results of such studies are needed in practice because there is an opportunity to improve the quality of motion cueing and the efficiency of using FFS for research and development of aircraft, as well as crew training.

The relevance of research into the optimization of the use of structural resources of DOF6 is due to the fact that, in addition to increasing the efficiency of the use of FFS, there is an opportunity to use DOF6 with jacks of a shorter length, and therefore to reduce the cost of its manufacture and operation.

Fig. 1. Full flight simulator with a six degrees-of-freedom motion system

2. Literature review and problem statement

The design of modern DOF6 flight simulators is based on the structure described in [1]. The article describes the DOF6 mechanism, which has six degrees of freedom, controlled in any combination by six jacks, each of which is grounded. Due to its

special design, this mechanism can form an elegant structure to simulate flight conditions during pilot training. Optimum use of structural resources of the Stewart platform will contribute to improving the quality of simulation of flight conditions.

In [2], the equation of the dynamics of the Stewart platform under the action of the forces applied to the rods of the jacks was derived. Direct and inverse dynamics problems are solved. To solve the inverse problem of dynamics, which is unstable, feedback is introduced. The control of displacements and velocities of jack rods, which leads to steady motion, is considered. Without accounting for the use of structural resources, the Stewart platform dynamics equation is incomplete and of limited use.

Paper [3] discusses the design of a flight simulator with variable stability. The simulator also provides a platform for researchers to understand the dynamics of the aircraft. The simulator is supplemented with optimization methods to adjust the control characteristics. Without solving the issue of optimal use of structural resources DOF6, the simulator has limited capabilities.

Study [4] reports an innovative architectural and structural application of the Stewart-Hoff platform. For each telescopic rack, the stability of various configurations was investigated. Self-collision of rack-rack, rack-roof, and roof-floor was investigated using physical and computational models. The path trajectory of the kinematic structure was studied from the point of view of the magnitude and type of motion. The final choice of the telescopic rack was based on the conclusions of parametric architectural and structural studies. Taking into account the issue of optimal use of structural resources DOF6 makes it possible to make a more optimal choice of a telescopic rack.

In [5], various options for the structural implementation of robotic motion platforms are considered and analyzed. On the basis of a parameterized simulation model, a study was conducted on the optimal location of the attachment points of the hinge joints in the upper motion platform. At the same time, minimization of power pairs of meters in the reactions of the corresponding resistances was chosen as an optimization criterion. Taking into account the criteria for optimizing the design resources of motion platforms can improve the efficiency of the location of the points of attachment of hinged joints in the upper motion platform.

In study [6], mathematical modeling of the AS-532 Cougar helicopter was performed using the Newton-Euler equation. The mathematical model uses force and torque equations that take into account the inertial properties of the system. The use of the motion system with the optimal use of DOF6 structural resources makes it possible to significantly improve the quality of modeling.

Paper [7] describes several basic elements of Stewart's platforms, presents an accurate original method of analytical geometry for determining the kinematic and dynamic parameters of a parallel motion structure. The method has a great advantage in that it is an accurate analytical method of calculation, and not an iterative-approximate one. But when using it, it is useful to take into account the structural resources of Stewart's platforms.

In [8], various options for the structural implementation of robotic motion platforms are considered and analyzed. On the basis of a parameterized simulation model, a study was conducted on the optimal location of the attachment points of the hinge joints in the upper motion platform. At the same time, minimization of power parameters in the reactions of the corresponding resistances was chosen as an optimization criterion. This criterion is partial due to the lack of consideration of the optimal utilization of structural resources.

In [9], a stability control system was designed for a medium-range jet using nonlinear dynamic inversion. The aircraft's control system is based on the existing autopilot, inheriting limited performance and safety protection. The simulator experiment showed the differences between the control qualities of the reference model and the designed controller in combination with the aircraft dynamics. Overcoming this difference is possible under the condition of using a motion system with optimal use of DOF6 structural resources.

Paper [10] reports a study of motion control automation of Stewart platforms. First, the design, kinematic modeling, and trajectory generation of the Stewart platform robot are analyzed, and direct kinematics and motion automation are considered. The effective calculation of direct kinematics in real time has been studied. This opens up the possibility of closing the positioning loop on the controller or implementing supervisors such as «tracking error». Further research could examine the impact of sequence planning to avoid collisions with objects within the workspace, taking into account tracking error feedback and optimal use of DOF6 structural resources.

The authors of [11] report a new controller intended for industrial areas, which improves the characteristics and accuracy of positioning systems based on Stewart platforms. The paper presents and experimentally validates sliding mode control for precise positioning of a Stewart platform. The precise platform positioning operation requires the coordinated control of six electromechanical jacks. The trajectory of the platform and the length of the jacks were calculated using the forward and inverse kinematics of the Stewart platform. A sliding mode control strategy is proposed for accurate positioning of the platform. This requires a priori knowledge of system uncertainty limits and system stability analysis. Taking into account the structural resources can contribute to a more accurate positioning of the Stewart platform.

Paper [12] describes a geometric approach for real-time direct kinematics of a general Stewart platform, which consists of two rigid bodies connected by six general serial manipulators. A very neat and simple differential relationship between the space of tasks and the space of connections is established. The proposed algorithm is accurate, reliable, and fast. Taking into account the structural resources of the Stewart platform in the proposed geometric approach can improve the accuracy of calculations.

It can be concluded that to date, the issue of optimizing the utilization of DOF6 structural resources has not been given enough attention. The reason for this may be that DOF6 has found wide application in various branches of mechanical engineering, in particular in robotics, and it is the application in these branches, and not in flight simulators, which is given the greatest attention.

The design of DOF6 is widely used in flight simulators, in particular in FFS. This application was developed by Redifon. In Ukraine, DOF6 are used on An-74TK-200 and An-148 flight simulators, and their use in flight simulators under construction is expected. Therefore, it can be stated that it is expedient to conduct a study on the optimization of the utilization of structural resources of DOF6 flight simulators.

3. The aim and objectives of the study

The purpose of this study is to determine ways to optimize the use of structural resources of DOF6. This makes it

possible to increase the efficiency of using FFS for training pilots, it becomes possible to use DOF6 with jacks of a shorter length, and therefore to reduce the cost of their manufacture and operation.

To achieve the goal, the following tasks were solved:

– to determine the movement of jacks depending on the required movements of DOF6 along degrees of freedom,

– to determine the coordinates of the point *O* of the beginning of the connected coordinate system *OXYZ* along the longitudinal axis *OX*,

– to determine the permissible movements of DOF6,

– to determine the maximum working ranges of DOF6 movements,

– to build the objective function and determine the optimal coordinates of the pitch and yaw axes.

4. The study materials and methods

4. 1. The object and hypothesis of the study

The object of our research is a six degrees-of-freedom motion system of the synergistic type.

Research based on the principles of theoretical mechanics showed the inadmissibility of using DOF6 with jacks 2 m long to motion cueing. Therefore, the main hypothesis of the study was to take into account the peculiarities of the pilot's perception of motion cues and their simulation on FFS.

In the study, the hypothesis was accepted that with more complex movements of jacks, necessary for the effective use of DOF6 structural resources, false motion cues would not occur.

In the study, the hypothesis of simplifying the operator of the transformation of the movement of DOF6 along individual degrees of freedom into the movement of jacks was adopted. Owing to this, it became possible to describe the coordinates of the pitch and yaw rotation axes with cubic spline functions.

Calculations were carried out using programs that we developed and written in the C programming language. Objective function minimization tasks were performed using the modified Nelder-Mead method.

4. 2. Determination of movements of jacks depending on the required movements of DOF6 along degrees of freedom

All six jacks are involved in the movement of DOF6 (Fig. 2) along any degree of freedom (except for roll movement, in which four jacks are involved). This leads to a strong interdependence of DOF6 movements along different degrees of freedom: movement along any of the degrees of freedom leads to a decrease in permissible movements along other degrees of freedom. The need to ensure the simultaneous movement of DOF6 along several degrees of freedom requires solving the problem of determining the movements of jacks depending on the necessary movements of DOF6 along degrees of freedom.

$$L_m = W_u \cdot S;$$

$$S \in S^*, \qquad (1)$$

where L_m is the length vector of jacks $L_m = \{l_k, k = \overline{1,6}\}$; W_u is the operator for converting the movement of DOF6 along individual degrees of freedom into the movement of jacks; S is the vector of necessary displacements of DOF6 along individual degrees of freedom $S = [x, y, z, \gamma, \theta, \psi]^T$, where x, y, z, γ, θ, ψ are, respectively, displacements of DOF6 along longitudinal, vertical, and lateral degrees freedom, roll, yaw and pitch; S^* is a vector of working ranges of DOF6 movements along individual degrees of freedom $S^* = [x^*, y^*, z^*, \gamma^*, \theta^*, \psi^*]^T$, where x^*, y^*, z^*, γ^*, θ^*, ψ^* are, respectively, the operating ranges of DOF6 movements along longitudinal, vertical, lateral degrees of freedom, roll, yaw and pitch.

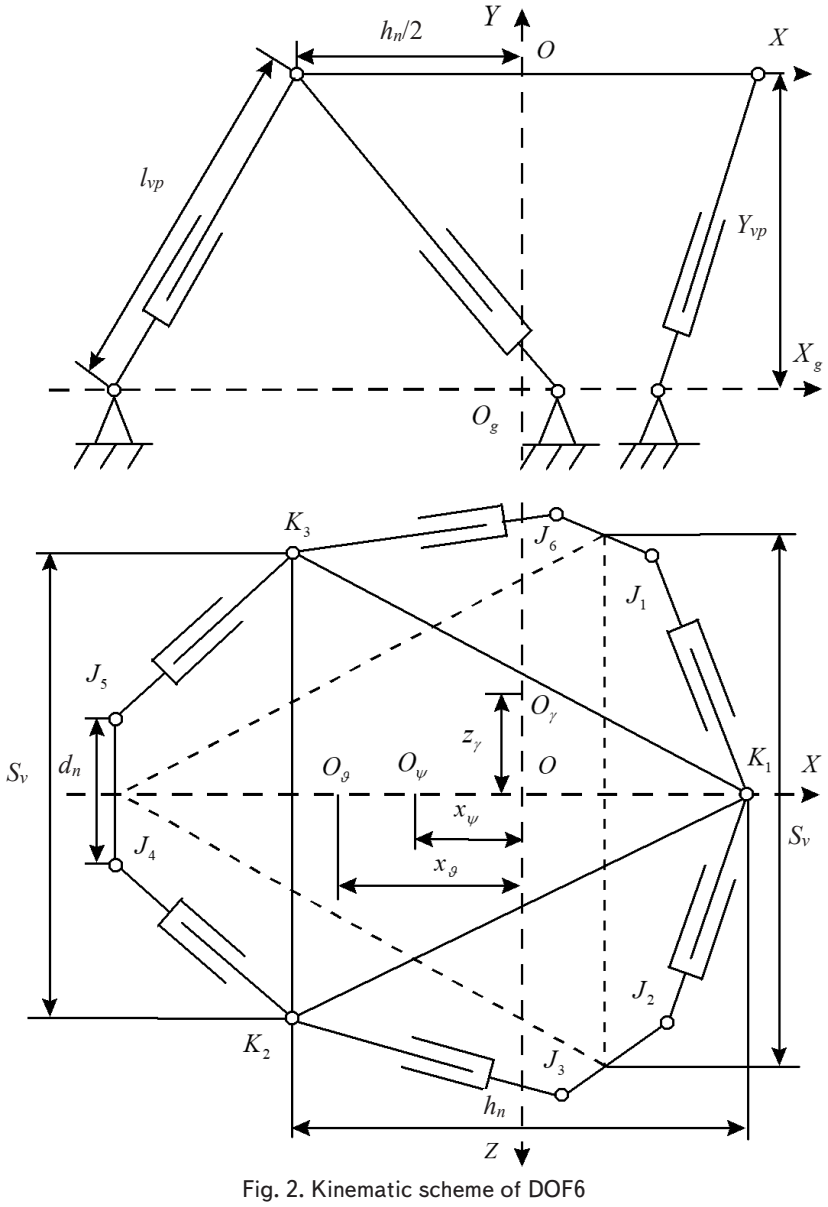

Fig. 2. Kinematic scheme of DOF6

To form the transformation operator W_u, we introduce (Fig. 2) the right-hand coordinate system *OXYZ* connected to DOF6. The origin of *OXYZ*, point *O* is in the plane of the centers of rotation of the upper hinges $K_1K_2K_3$, and the axes *OX, OY* and *OZ* are parallel to the corresponding axes of the plane. We also introduce the normal Earth coordinate system $O_gX_gY_gZ_g$. The $O_gX_gY_gZ_g$ beginning point O_g coincides with the projection of point *O* onto the plane of the centers of rotation of the lower hinges of DOF6 $J_1J_2J_3J_4J_5J_6$. The condition is that the movements of DOF6 jacks are equal, and the O_gX_g, O_gY_g and O_gZ_g axes are parallel to the axes *OX, OY*, and *OZ*, respectively. The angular orientation of the connected coordinate system *OXYZ* is determined by the angles of roll γ, yaw ψ, and pitch θ.

The vectors of the coordinates of the centers of rotation of the upper hinges of the jacks in the Earth coordinate system $O_gX_gY_gZ_g$ along the axes O_gX_g, O_gY_g and O_gZ_g $x_v=\{x_{vk}\}$, $y_v=\{y_{vk}\}$, $z_v=\{z_{vk}\}$, where x_{vk}, y_{vk}, z_{vk} are, respectively, the coordinates of the centers of rotation of *k*-th upper hinges of jacks in the Earth coordinate system $O_gX_gY_gZ_g$ along the O_gX_g, O_gY_g and O_gZ_g axes are described by the expression:

$$\begin{vmatrix} x_v \\ y_v \\ z_v \end{vmatrix} = \begin{vmatrix} x \\ y \\ z \end{vmatrix} + \mathrm{A}_{tm} \begin{vmatrix} x_{vo} \\ y_{vo} \\ z_{vo} \end{vmatrix}, \quad (2)$$

where x_{vo}, y_{vo}, z_{vo} are, respectively, the vectors of the centers of rotation of the upper hinges of jacks in the connected coordinate system *OXYZ* along the axes *OX*, *OY* and *OZ* $x_{vo}=\{x_{vok}\}$, $y_{vo}=\{y_{vok}\}$, $z_{vo}=\{z_{vok}\}$, where x_{vok}, y_{vok}, z_{vok} are, respectively, the coordinates of the centers of rotation of the *k*-th upper hinges of jacks in the connected coordinate system *OXYZ* along the *OX*, *OY* and *OZ* axes; A_{tm} is the transformation matrix from the connected coordinate system *OXYZ* to the Earth coordinate system $O_gX_gY_gZ_g$ [13]:

$$A_{tm} = \begin{pmatrix} \cos\psi\cos\theta & \sin\theta & -\cos\theta\sin\psi \\ -\sin\theta\cos\psi\cos\gamma+\sin\psi\sin\gamma & \cos\theta\cos\gamma & \cos\psi\sin\gamma+\sin\theta\sin\psi\cos\gamma \\ \sin\theta\cos\psi\sin\gamma+\sin\psi\cos\gamma & -\cos\theta\sin\gamma & \cos\psi\cos\gamma-\sin\theta\sin\psi\sin\gamma \end{pmatrix}. \quad (3)$$

Quadratic approximation implies replacing the trigonometric functions of the angles with the angles themselves and preserving in (3) the values of only the first and second order of smallness. Considering the angles to be small and taking into account the small range of their change, in the scalar form the coordinates of the centers of rotation of the upper hinges of jacks in the Earth coordinate system $O_gX_gY_gZ_g$ (3) are described by the equations:

$$\begin{aligned} x_{vk} &= x + x_{vk}[1-0.5(\psi^2+\theta^2)] + z_{vk}(\theta_y+\psi); \\ y_{vk} &= y + x_{vk}\theta - z_{vk}\gamma + Y_{vp}; \\ z_{vk} &= z - x_{vok}\psi + z_{vok}[1-0.5(\psi^2+\gamma^2)], \ k=\overline{1.6}, \end{aligned} \quad (4)$$

where Y_{vp} is the coordinate of the centers of rotation of the upper hinges of the jacks along the vertical axis *OY* in the initial position of DOF6, x_{nk}, z_{nk} are the coordinates of the centers of rotation of the *k*-th lower hinges of the jacks in the Earth coordinate system $O_gX_gY_gZ_g$ along the O_gX_g and O_gZ_g axes; l_{vp} is the average length of the jacks, which corresponds to the initial position of DOF6 and is equal to half the working stroke of the rods of the jacks $l_{vp}=(l_{\max}-l_{\min})/2$. In the last equation, $l_{\max}$, $l_{\min}$ are, respectively, the length of the rods of jacks with the rod maximally extended and maximally retracted. These lengths are defined as the distances between the upper and lower centers of rotation of the hinges of jacks along the direction of the jack when the rod is fully extended and fully retracted.

The coordinates of the centers of rotation of the lower hinges of jacks in the Earth coordinate system $O_gX_gY_gZ_g$ and the coordinates of the centers of rotation of the upper hinges of jacks in the connected coordinate system *OXYZ* are determined by two variables (Fig. 2):

– the side of the triangle between the lower and upper supports $S_n=S_v$;

– the distance between the supports of the lower hinges d_n and using the formulas:

$$x_n = \begin{vmatrix} \sqrt{3}(S_n+4d_n)/12 \\ \sqrt{3}(S_n+4d_n)/12 \\ \sqrt{3}(S_n+2d_n)/12 \\ \sqrt{3}(S_n+2d_n)/12 \\ \sqrt{3}(5S_n+2d_n)/12 \\ \sqrt{3}(5S_n+2d_n)/12 \end{vmatrix}; \ z_n = \begin{vmatrix} -0.5S_n \\ 0.5S_n \\ 0.5(S_n+d_n) \\ 0{,}5d_n \\ -0{,}5d_n \\ -0.5(S_n+d_n) \end{vmatrix};$$

$$x_{vo} = \begin{vmatrix} \sqrt{3}S_n/4 \\ \sqrt{3}S_n/4 \\ -\sqrt{3}S_n/4 \\ -\sqrt{3}S_n/4 \\ -\sqrt{3}S_n/4 \\ -\sqrt{3}S_n/4 \end{vmatrix}; \ z_{vo} = \begin{vmatrix} 0 \\ 0 \\ 0.5S_v \\ 0.5S_v \\ -0.5S_v \\ -0.5S_v \end{vmatrix}; \quad (5)$$

Movements of jacks are calculated by the formula:

$$l_k = \sqrt{(x_{vk}-x_{nk})^2 + y_{vk}^2 + (z_{vk}-z_{nk})^2} - l_{vp}, \ k=\overline{1,6}. \quad (6)$$

(4) to (6) is a system of nonlinear equations that fully determines the dependence of the movements of jacks on the movement of DOF6 along individual degrees of freedom (1).

4. 3. Determination of the coordinates of the point *O* of the beginning of the connected coordinate system *OXYZ* along the longitudinal axis *OX*

The effectiveness of the use of structural resources of DOF6 is determined by the degree of use of its permissible movements along degrees of freedom. It depends on many factors, including the initial position *O* of the connected coordinate system *OXYZ* and the direction of the longitudinal axis *OX*. These values are determined by the coordinates of the centers of rotation of the lower and upper hinges of jacks (5). The selection criterion is the best position of point *O* of the critical jack, that is, a jack whose rod is in the maximum extended or maximum retracted position. For this purpose, the relative movement of the critical jack is estimated along the *j*-th degree of freedom:

$$\overline{l_{krj}} = \min_{x_0} \max \left| \frac{\theta l_k}{\theta s} \right|, \; k = \overline{1.6}, j = \overline{1.6}, \tag{7}$$

where x_0 is the coordinate of the point O of the beginning of the connected coordinate system $OXYZ$ along the longitudinal axis OX. x_0 solves the minimax problem.

4. 4. Determination of permissible movements of DOF6

When the limit position is reached by at least one jack, movement of DOF6 along this degree of freedom is impossible without movement in the opposite direction or along another degree of freedom. However, during angular movements of DOF6, the axis of rotation can be brought closer to the jack, which will reach the limit position first. This makes it possible to reduce the movement of this jack or even eliminate it if the axis of rotation is located in the center of rotation of the hinge. It is important to note that in this case the jacks perform a more complex movement than with the traditional approach.

The axis of rotation of the aircraft is located in the center of gravity, which is at a considerable distance from the cabin. Motion cues on flight simulators do not reach the values of real motion cues. The displacement of coordinates of the pitch and yaw axes along the direction of the center of gravity of the aircraft provides an increase in the linear motion cues of DOF6 due to angular movements. Therefore, if the jacks have not reached their limits, it is possible to shift the coordinates of the pitch and yaw axes along the longitudinal axis OX in such a way that they approach the coordinate of the center of gravity of the aircraft x_g:

$$x_\theta \to x_g; x_\psi \to x_g. \tag{8}$$

To this end, the coordinates of the pitch and yaw axes along the longitudinal axis OX are set by linear dependences:

$$x_\vartheta = \begin{cases} x_\vartheta^- \;\Big|\; \vartheta \le -\vartheta^*; \\ x_\vartheta^- + \dfrac{x_\vartheta^+ - x_\vartheta^-}{2\vartheta^*}\left(\vartheta + \vartheta^*\right) \Big| -\vartheta^* < \vartheta < \vartheta^*; \\ x_\vartheta^+ \;\Big|\; \vartheta \ge \vartheta^*, \end{cases}$$

$$x_\psi = \begin{cases} x_\psi^- \;\Big|\; \vartheta \le -\vartheta^*; \\ x_\psi^- + \dfrac{x_\psi^+ - x_\psi^-}{2\vartheta^*}\left(\vartheta + \vartheta^*\right) \Big| -\vartheta^* < \vartheta < \vartheta^*; \\ x_\psi^+ \;\Big|\; \vartheta \ge \vartheta^*, \end{cases} \tag{9}$$

where $-\theta$, θ are, respectively, the maximum negative and positive value of the operating pitch range of DOF6; x_ϑ^-, x_ϑ^+, x_ψ^-, x_ψ^+ are, respectively, the coordinates of the pitch and yaw axes of DOF6 along the longitudinal axis OX, which correspond to the extreme negative and positive values of the operating range of the DOF6 pitch.

In (9), the movement of DOF6 along pitch and yaw are connected linearly. This makes it possible to calculate the coordinates of the centers of rotation of the hinges of the upper jacks according to the formulas:

$$x_{vk} = x + x_{vok} - 0.5\left[\begin{matrix}\left(x_{vok} - x_\theta\right)\psi^2 + \\ +\left(x_{vok} - x_\psi\right)\theta^2\end{matrix}\right] + z_{vok}\left(\theta\gamma + \psi\right);$$

$$y_{vk} = y + \left(x_{vok} - x_\theta\right)\theta - z_{vok}\gamma + Y_{vp}; \tag{10}$$

$$z_{vk} = z - \left(x_{vok} - x_\psi\right)\psi + z_{vok}\left[1 - 0.5\left(\psi^2 + \gamma^2\right)\right], \; k = \overline{1.6}.$$

The problem of determining the permissible movements of DOF6 is reduced to extreme:

$$\overline{s} = \max s,$$

$$L_m \in \Omega_l, \tag{11}$$

where $\overline{s}$, s are the permissible displacement and displacement of DOF6, respectively; Ω_l is area of determination of the lengths of jacks.

4. 5. Determination of the maximum operating ranges of DOF6 movement

An important component for the maximum utilization of DOF6 structural resources is task of determining the maximum working ranges of DOF6 movement. In general, this comes down to an extreme problem:

$$\sum_{i=1}^{7} s_i^* \to \max,$$

$$L_m \in \Omega_l,$$

$$-s_i^* \le s_i \le s_i^*,$$

where s_i^*, s_i, are, respectively, the i-th operating range and the i-th displacement of DOF6 along individual degrees of freedom $\{s_i^*\} = [x^*, y^*, z^*, \gamma^*, \theta^*, \psi^*]$, $\{s_i\} = [x, y, z, \gamma, \theta, \psi]$, where x^*, y^*, z^*, γ^*, θ^*, ψ^*, x, y, z, γ, θ, ψ are, respectively, working ranges of movement and movement of DOF6 for motion cueing along the longitudinal, vertical, and lateral degrees of freedom, roll, yaw; γ_Σ^*, γ_Σ are, respectively, the operating range and displacement of DOF6 for the motion cueing along roll and static motion cueing along the lateral degree of freedom; θ^*, θ are, respectively, the operating range and displacement of DOF6 for the motion cueing along the pitch and the static motion cueing along the longitudinal degree of freedom.

The set of kinematically possible displacements of DOF6 is given in the form of a region of possible positions in an n-dimensional space of n composite coordinates. The developed method of motion cueing requires the following minimum ranges of DOF6 movements (when using traditional methods of motion cueing, much larger ranges of DOF6 movements are required):

– to motion cueing along the longitudinal, vertical, and lateral degrees of freedom $x_{\min} = y_{\min} = z_{\min} = 0.4$ m;

– to motion cueing along roll $\gamma_{\min} = 5$ degrees;

– for motion cueing along roll and static motion cueing along the lateral degree of freedom $\gamma_{\Sigma\min} = 10$ degrees;

– to motion cueing along yaw $\psi_{\min} = 4$ degrees;

– for modeling aircraft pitch and static motion cueing along the longitudinal degree of freedom $\theta_{\min} = 9$ degrees.

To effectively solve the problem of determining the working ranges of movement of DOF6, it is necessary to take into account the peculiarities of piloting and perception of motion cues along the degree of freedom. The geometric meaning of this problem consists in fitting into the five-dimensional domain the possible positions of DOF6 $\tilde{U}$ in turn of three parallelepipeds, namely:

– parallelepiped $\tilde{P}_{s1}$, the length of one edge of which is equal to the minimum necessary range of movement of DOF6 along yaw, and the length of the other two edges is not less than the minimum necessary ranges of movement of DOF6 along pitch and longitudinal degrees of freedom:

$$\tilde{P}_{s1}=\left\{(y,\theta,\psi)\middle|\, x^*\geq x_{\min},\theta^*\geq\theta_{\min},-\psi_{\min}\leq\psi\leq\psi_{\min}\right\};$$

– parallelepiped $\tilde{P}_{s2}$, the length of one edge of which is equal to the minimum necessary range of movement of DOF6 along roll, and the length of the other two edges is not less than the minimum necessary ranges of movement of DOF6 along pitch and vertical degrees of freedom:

$$\tilde{P}_{s2}=\left\{(y,\theta,\gamma)\middle|\, y^*\geq y_{\min},\theta^*\geq\theta_{\min},-\gamma_{\min}\leq\gamma\leq\gamma_{\min}\right\};$$

– a hyper parallelepiped, the lengths of the two edges of which are equal to the minimum necessary ranges of movement of DOF6, along roll and yaw. And the lengths of its other two edges are not less than the minimum necessary ranges of movement of DOF6 along pitch and lateral degrees of freedom:

$$\tilde{P}_{s3}=\left\{\begin{matrix}(y,\theta,\gamma_\Sigma,\psi)\middle|\, z^*\geq z_{\min},\theta^*\geq\theta_{\min},\\ -\gamma_{\Sigma\min}\leq\gamma_\Sigma\leq\gamma_{\Sigma\min},-\psi_{\min}\leq\psi\leq\psi_{\min}\end{matrix}\right\}.$$

The minimum necessary ranges of movements of DOF6 along roll and yaw are sufficient for a high-quality motion cueing of a non-maneuverable aircraft. Therefore, the working ranges of movements of DOF6 along pitch, longitudinal, lateral, and vertical degrees of freedom are sought:

$$x^*+y^*+z^*+\theta^*\to\max,$$

$$\tilde{P}_{s1}\subset\tilde{U},\tilde{P}_{s2}\subset\tilde{U},\tilde{P}_{s3}\subset\tilde{U}. \qquad (12)$$

Criterion (12) guarantees that the sum of the operating ranges of DOF6 movements along pitch, longitudinal, lateral, and vertical degrees of freedom will be maximal.

4. 6. Construction of the objective function and determination of the optimal coordinates of the pitch and yaw axes

With the maximum use of the structural resources of DOF6, when the coordinates of the pitch and yaw axes are shifted in such a way as to ensure the maximum working ranges of movements of DOF6, the task of their determination is reduced to an extreme problem:

$$x^*+y^*+z^*+\theta^*\to\max,$$

$$\tilde{P}_{s1}\subset\tilde{U},\tilde{P}_{s2}\subset\tilde{U},\tilde{P}_{s3}\subset\tilde{U},x_\theta\to x_g,x_\psi\to x_g. \qquad (13)$$

It is obvious that the structural resources of DOF6 are determined by the discrepancy between the permissible movement and the working range of movements. It is desirable that the structural resource of DOF6 is fully used and the values of permissible movements of DOF6 are equal to the values of the corresponding working ranges of movements. The criteria for evaluating the structural resources of DOF6 along the longitudinal, vertical, and lateral degrees of freedom are calculated according to the formulas:

$$J_x=\int_{-\theta^*}^{\theta^*}\left|\bar{x}(\theta)-x^*\right|^2\mathrm{d}\theta;$$

$$J_y=\int_{-\theta^*}^{\theta^*}\left|\bar{y}(\theta)-y^*\right|^2\mathrm{d}\theta;$$

$$J_z=\int_{-\theta^*}^{\theta^*}\left|\bar{z}(\theta)-z^*\right|^2\mathrm{d}\theta.$$

To improve the quality of motion cueing and the efficiency of using the structural resource of DOF6, the working range of movements of DOF6 along the pitch is divided into subintervals, the coordinates of the pitch and yaw axes are described by cubic spline functions:

$$x_\vartheta(\theta)=$$
$$=\begin{cases}x_\theta^- \ \middle|\ \theta\leq\theta_{\theta1}=-\theta^*;\\ \left[\begin{matrix}M_{\theta i}\left(\theta_{\theta(i+1)}-\theta\right)^3+\\ +M_{\theta(i+1)}\left(\theta-\theta_{\theta i}\right)^3+\\ +\left(6x_{\theta i}-M_{\theta i}h_{\theta i}^2\right)\times\\ \times\left(\theta_{\theta(i+1)}-\theta\right)+\\ +\left(6x_{\theta(i+1)}-M_{\theta(i+1)}h_{\theta i}^2\right)\times\\ \times\left(\theta-\theta_{\theta i}\right)\end{matrix}\right]/6h_{\theta i}\ \middle|\ \theta_{\theta i}<\theta\leq\theta_{\theta(i+1)},\\ x_\theta^+ \ \middle|\ \theta>\theta_{\theta n\theta}=\theta^*;\end{cases}$$
$$i=\overline{1,n_\theta-1},$$
$$x_\psi(\theta)=$$
$$=\begin{cases}x_\psi^- \ \middle|\ \theta\leq\theta_{\psi1}=-\theta^*;\\ \left[\begin{matrix}M_{\psi i}\left(\theta_{\psi(i+1)}-\theta\right)^3+\\ +M_{\psi(i+1)}\left(\theta-\theta_{\psi i}\right)^3+\\ +\left(6x_{\psi i}-M_{\psi i}h_{\theta i}^2\right)\times\\ \times\left(\theta_{\psi(i+1)}-\theta\right)+\\ +\left(6x_{\psi(i+1)}-M_{\psi(i+1)}h_{\psi i}^2\right)\times\\ \times\left(\theta-\theta_{\psi i}\right)\end{matrix}\right]/6h_{\psi i}\ \middle|\ \theta_{\psi i}<\theta\leq\theta_{\psi(i+1)},\\ x_\psi^+ \ \middle|\ \theta>\theta_{\psi n\psi}=\theta^*,\end{cases}$$
$$i=\overline{1,n_\psi-1}, \qquad (14)$$

where $\theta_{\theta i}$, $\theta_{\psi i}$ is, respectively, the i-th point of division of the working pitch range of DOF6 into subintervals $i[\theta_{\psi i};\theta_{\psi(i+1)}]$, $i=\overline{1,n_\psi-1}$; i is the index of the dividing point of the working pitch range of DOF6; n_θ, n_ψ are, respectively, the number of points of division of the working pitch range of DOF6 into subintervals $[\theta_{\psi i};\theta_{\psi(i+1)}]$, $i=\overline{1,n_\psi-1}$; $x_{\psi i}$, $x_{\theta i}$ are respectively, the coordinates of the pitch and yaw axis of DOF6 along the longitudinal axis OX at the i-th point of division of the working range of DOF6 pitch into subintervals $[\theta_{\psi i};\theta_{\psi(i+1)}]$, $i=\overline{1,n_\psi-1}$; $M_{\psi i}=\ddot{x}_\psi\left(\theta_{\psi i}\right)$, $M_{\theta i}=\ddot{x}_\theta\left(\theta_{\theta i}\right)$ are constant coefficients; $h_{\theta i}=\theta_{\theta(i+1)}-\theta_{\theta i}$, $h_{\psi i}=\theta_{\psi(i+1)}-\theta_{\psi i}$ are partition steps, and shifted along the direction of the center of gravity of the aircraft (6). The values of the coordinates of the pitch and yaw axes along the longitudinal axis OX at the points of division of DOF6 operating range $\{x_\theta\}$ and $\{x_\psi\}$ and the constant coefficients of the cubic spline functions $\{M_\theta\}$ and $\{M_\psi\}$ are found.

Therefore, the task of maximum use of structural resources of DOF6 is reduced to an extreme problem:

$$J_x+J_y+J_z\to\min;\begin{pmatrix}L_m\in\Omega_l;\bar{x}(\theta)\geq x^*;\bar{y}(\theta)\geq y^*;\\ \bar{z}\geq z^*;x_\theta(\theta)\to x_g;x_\psi(\theta)\to x_g;\\ -\theta^*\leq\theta\leq\theta^*;-\gamma^*\leq\gamma\leq\gamma^*;\\ -\gamma_\Sigma^*\leq\gamma_\Sigma\leq\gamma_\Sigma^*;-\psi^*\leq\psi\leq\psi^*\end{pmatrix}, \qquad (15)$$

where L_m, $\bar{x}$, $\bar{y}$, $\bar{z}$, x_θ, x_ψ, γ, γ_Σ, ψ are variables whose change solves the optimization problem.

The above criterion takes into account the peculiarities of motion cueing and solves the problem of maximum utilization of structural resources of DOF6.

5. Results of investigating the optimal utilization of DOF6 structural resources

5. 1. Determination of movements of jacks depending on the required movements of DOF6 along degrees of freedom

The calculated values of the coordinates of the lower and upper hinges of jacks of DOF6 with a length of 1.5 m (DOF6-1.5) are given in Table 1.

Table 1

Coordinates of the centers of rotation of the joints of jacks DOF6-1.5

Degrees of freedom	Jacks					
	1	2	3	4	5	6
z_{vo}, m	0	0	2.062	2.062	−2.062	−2.062
x_{vo}, m	1.785744	1.785744	−1.785744	−1.785744	−1.785744	−1.785744
z_n, m	−2.062	2.062	2.444	0.382	−0.382	−2.444
x_n, m	1.036344	1.036344	0.3747	−3.196789	−3.196789	0.3747
y_{vp}, m	2.790888					
l_{vp}, m	3.55					

Table 2 gives the results of calculations according to formula (7) of the relative displacements of the critical jacks of the DOF6 with the length of the jack rods of 1.5 m (DOF6-1.5) at the location of the point *O* of the beginning of the connected coordinate system.

Table 2

The relative displacement of the critical jack DOF6-1.5

Center of gravity	$\bar{l}_{krx}$	$\bar{l}_{kry}$	$\bar{l}_{krz}$	$\bar{l}_{kr\gamma}$, degree/m	$\bar{l}_{kr\psi}$, degree/m	$\bar{l}_{kr\theta}$, degree/m
$h_{n/2}$	0.532	0.830	0.665	0.0306	0.0321	0.0281
$h_{n/3}$	0.532	0.830	0.665	0.0306	0.0260	0.0333

These calculation results show the influence of the position of the beginning point *O* of the connected coordinate system on the relative displacement of the critical jack during DOF6 movements along linear and angular degrees of freedom.

5. 2. Determination of the coordinates of the point *O* of the beginning of the connected coordinate system *OXYZ* along the longitudinal axis *OX*

The calculation of permissible movements of DOF6-1.5 at the positions of the beginning point O of the connected coordinate system *OXYZ* at 1/2 and 1/3 of the height of the triangle of DOF6 (Fig. 2) is given in Table 3.

Table 3

Permissible movements of DOF6

Degree of freedom	DOF6	
	$h_{n/3}$	$h_{n/2}$
$\bar{x}$, m	−1.09; 1.40	−1.09; 1.40
$\bar{y}$, m	−1.05; 0.91	−1.05; 0.91
$\bar{z}$, m	−1.12; 1.12	−1.12; 1.12
$\bar{\gamma}$, degree	−25.3; 25.3	−25.3; 25.3
$\bar{\psi}$, degree	−29.7; 29.7	−23.8; 23.8
$\bar{\vartheta}$, degree	−24.1; 23.2	−27.4; 27.5

The values of permissible displacements of DOF6 serve as a basis for choosing the best position of the beginning point *O* of the connected coordinate system DOF6-1.5: the greater the permissible movement of DOF6 along degrees of freedom, the better the position of the beginning point *O* of the connected coordinate system.

5. 3. Determination of permissible movements of DOF6

The results of calculations of the working ranges of displacements of DOF6 (12) with the traditional approach, which were carried out by the modified method of the deformable polyhedron, are given in Table 4.

Table 4

Operating ranges of movement DOF6 (traditional approach)

Degree of freedom	DOF6-1	DOF6-1 (II)	DOF6-1.5
$\bar{x}$, m	0.52	0.52	0.76
$\bar{y}$, m	0.27	0.29	0.38
$\bar{z}$, m	0.33	0.33	0.44
$\bar{\theta}$, degree	11.4	11.4	12

The results of the calculations, which are given in Table 4, show the sufficiency or insufficiency of the operating ranges of DOF6 movements along individual degrees of freedom for motion cueing.

5. 4. Determination of the maximum operating ranges of DOF6 movement

A search was performed for the working ranges of DOF6 movements along pitch, longitudinal, vertical, and lateral degrees of freedom, the dependence of the coordinates of the pitch and yaw axes along the pitch angle. The results of solving problem (13) are given in Table 5.

Table 5

Operating ranges of DOF6 movement

Degrees of freedom	Traditional approach	Developed approach
$\bar{x}$, m	0.76	0.78
$\bar{y}$, m	0.38	0.49
$\bar{z}$, m	0.44	0.55
$\bar{\theta}$, degree	12	12

Thus, with the traditional approach, the permissible positive vertical displacement of DOF6 $\overline{y}^{+(-\vartheta)}$ is less than the other permissible vertical displacement of DOF6. This determines the working range of movement of DOF6 along the vertical degree of freedom. Similar ratios hold for other degrees of freedom. In particular, the working range of DOF6 displacement along the pitch in the traditional approach is determined by the allowable displacements of DOF6 along the lateral degree of freedom, and there is an unused structural resource of DOF6 along the longitudinal and vertical degrees of freedom.

With the maximum utilization of DOF6 structural resources (Fig. 3, 4, curve 1), positive and negative displacements of DOF6 vertically, corresponding to the extreme negative and positive values of the working range of DOF6 pitch, are practically the same. Almost the same negative and positive permissible movements of DOF6 along the lateral degree of freedom correspond to negative and positive values of the working range of DOF6 pitch.

Thus, with the maximum utilization of the structural resources of DOF6, it is possible to obtain larger working ranges of DOF6 movements (Fig. 3, 4, curves 3).

5. 5. Determination of optimal coordinates of the pitch and yaw axes

Analysis of the coordinates of the pitch and yaw axes, calculated when determining the operating ranges of DOF6 movements (Fig. 5, curve 2), shows that they differ significantly from the coordinates of similar aircraft axes (curve 1).

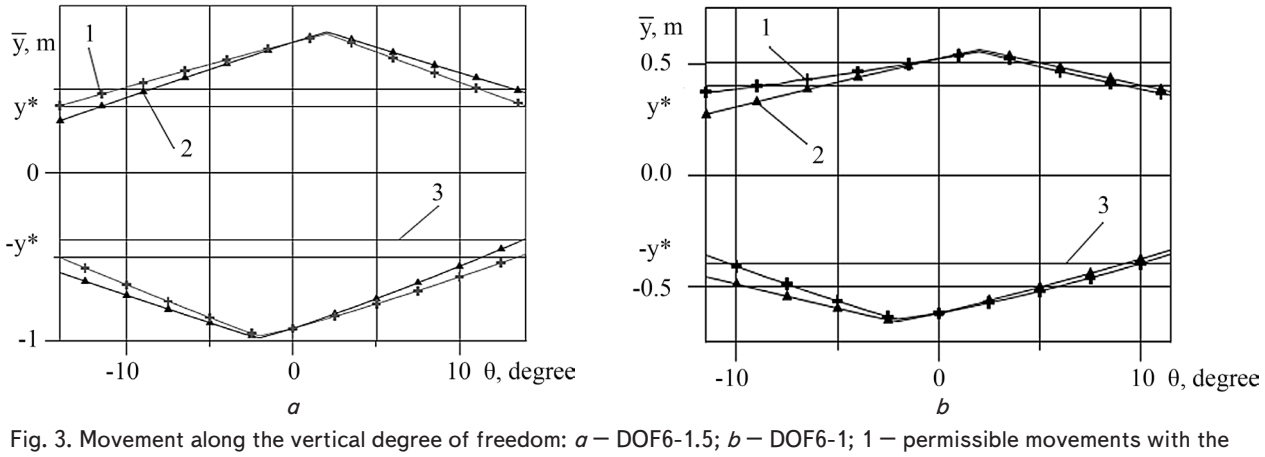

Fig. 3. Movement along the vertical degree of freedom: *a* — DOF6-1.5; *b* — DOF6-1; 1 — permissible movements with the developed approach; 2 — permissible movements with the traditional approach; 3 — maximum working ranges of movements

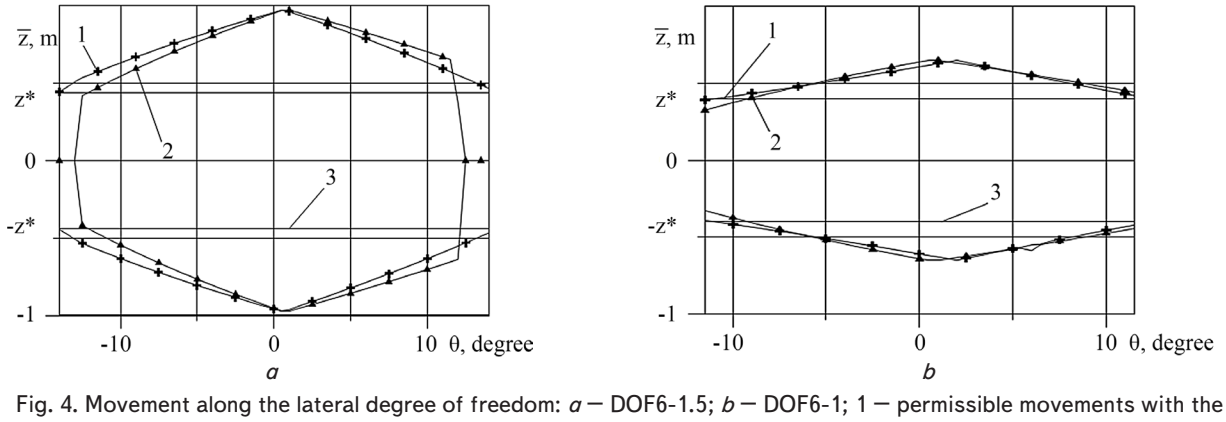

Fig. 4. Movement along the lateral degree of freedom: *a* — DOF6-1.5; *b* — DOF6-1; 1 — permissible movements with the developed approach; 2 — permissible movements with the traditional approach; 3 — maximum working ranges of movements

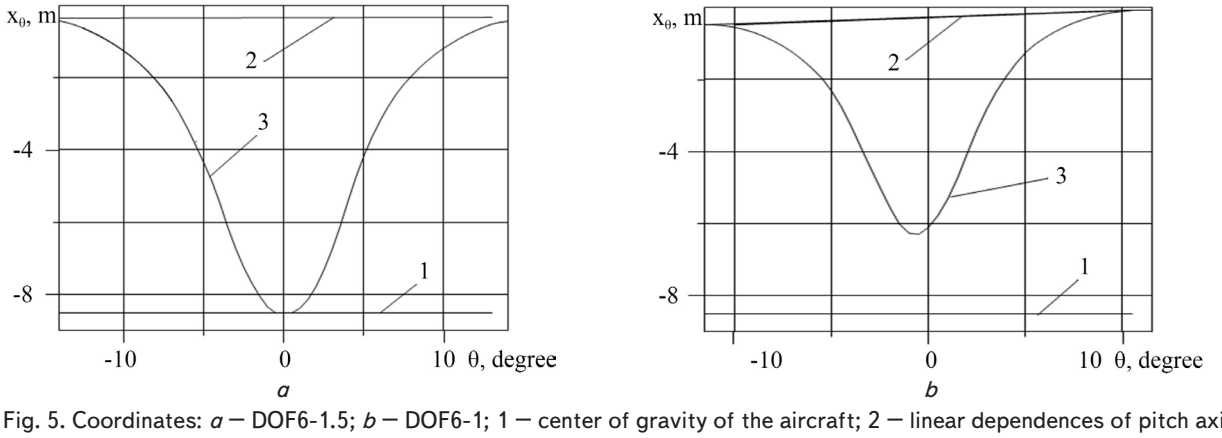

Fig. 5. Coordinates: *a* — DOF6-1.5; *b* — DOF6-1; 1 — center of gravity of the aircraft; 2 — linear dependences of pitch axis coordinates; 3 — dependences of pitch axis coordinates are described by cubic spline functions

On the other hand, as can be seen from Fig. 3, 4, the structural resource of DOF6 is not fully used.

The results of calculations (15) carried out by the deformation polyhedron method are shown in Fig. 5–8 (curves 2).

The movements of the most characteristic 2nd and 3rd jacks of DOF6-1.5 with a sinusoidal program signal with an amplitude of 14 degrees and a frequency of 0.2 Hz are shown in Fig. 9.

Fig. 9 shows the change in the nature of the movement of jacks with the developed approach.

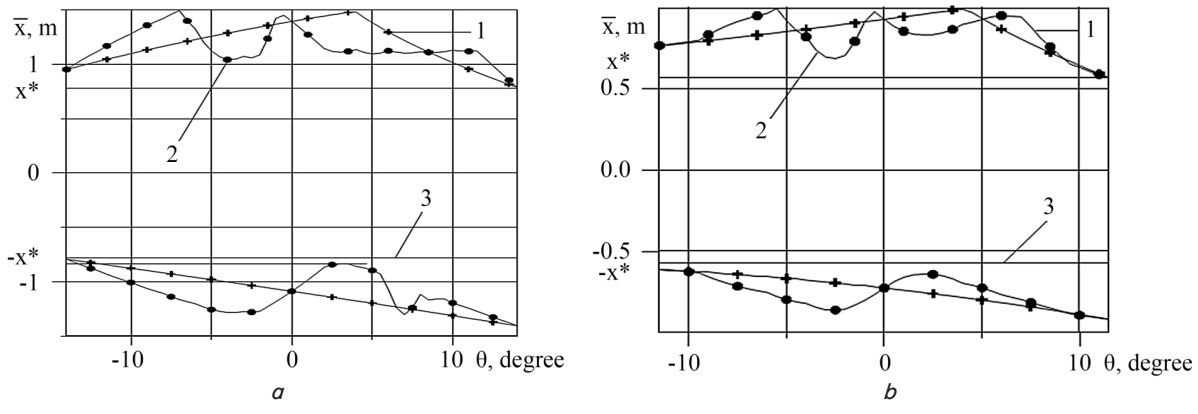

Fig. 6. Movement along the longitudinal degree of freedom:
a – DOF6-1.5; *b* – DOF6-1; 1 – permissible movements with linear dependence of coordinates of pitch and yaw axes;
2 – permissible displacements with cubic spline functions of coordinates of the pitch and yaw axes;
3 – maximum working ranges of movements

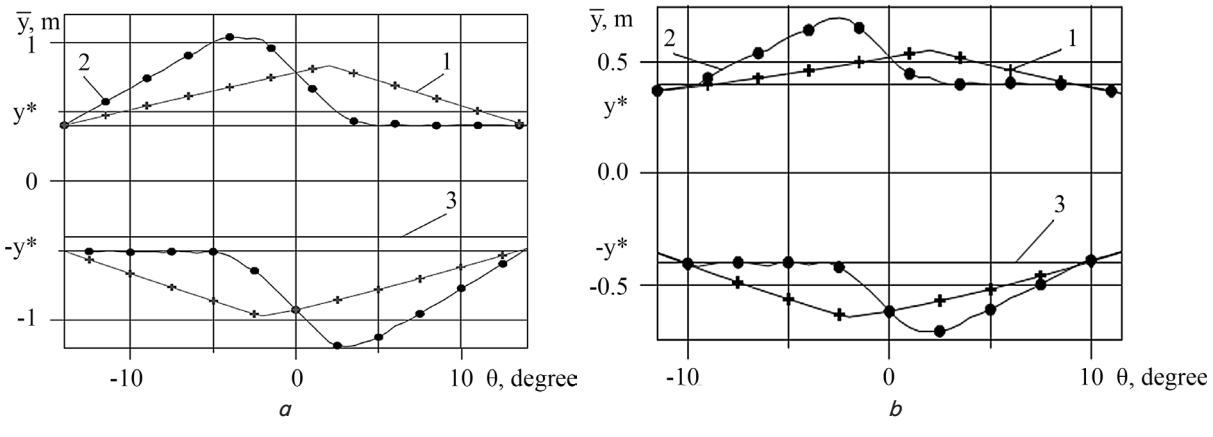

Fig. 7. Movement along the vertical degree of freedom:
a – DOF6-1.5; *b* – DOF6-1; 1 – permissible movements with linear dependence of coordinates of pitch and yaw axes;
2 – permissible displacements with cubic spline functions of coordinates of the pitch and yaw axes;
3 – maximum working ranges of movements

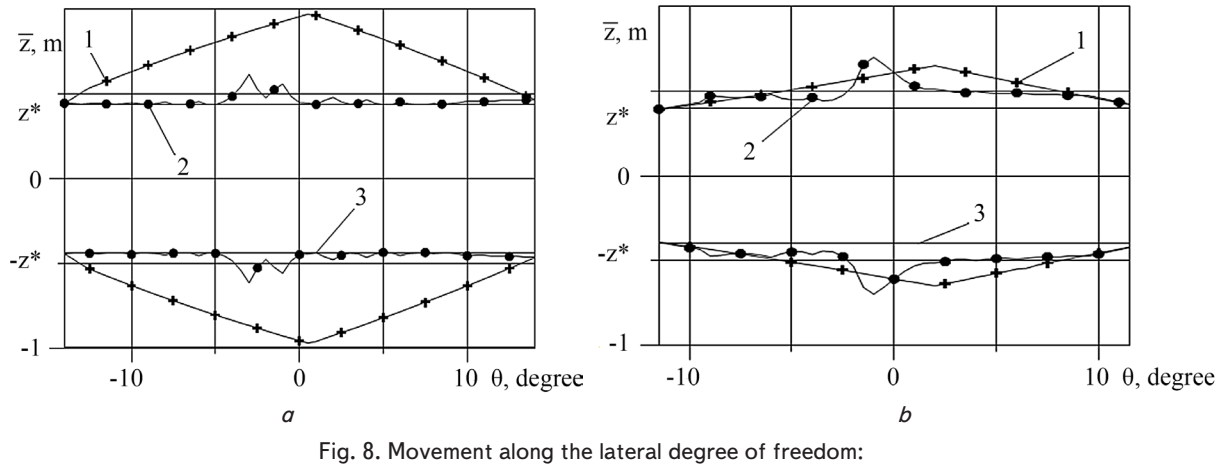

Fig. 8. Movement along the lateral degree of freedom:
a – DOF6-1.5; *b* – DOF6-1; 1 – permissible movements with linear dependence of coordinates of pitch and yaw axes;
2 – permissible displacements with cubic spline functions of coordinates of the pitch and yaw axes;
3 – maximum working ranges of movements

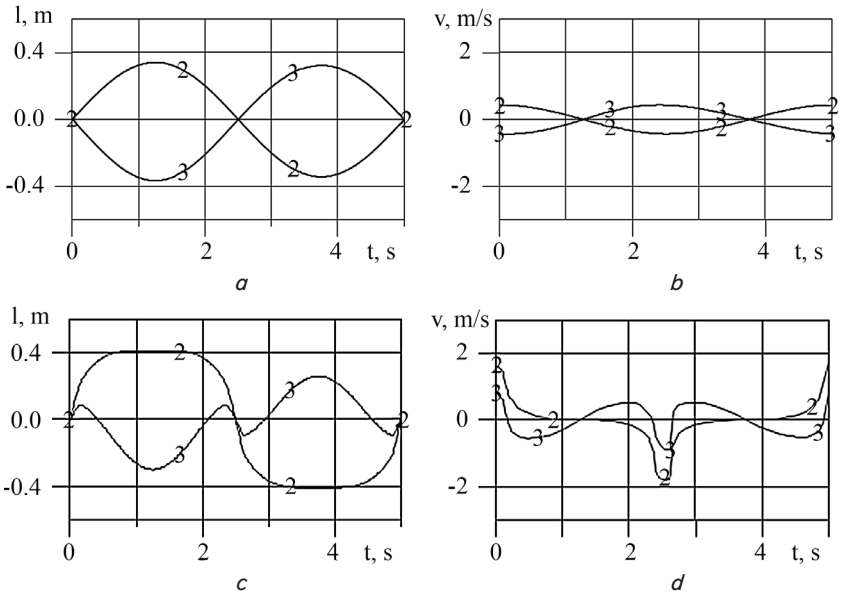

Fig. 9. Movement and speed of jacks: *a* — movement with the traditional approach; *b* — speed with the traditional approach; *c* —movement with the developed approach; *d* — speed with the developed approach; 2 — 2nd jack; 3 — 3rd jack

6. Discussion of results of the study on determining the optimal utilization of DOF6 structural resources

– the position of the beginning point *O* of the connected coordinate system *OXYZ* does not affect the relative movement of the critical jack during the movements of DOF6 along the linear degrees of freedom;

– due to the symmetry of DOF6 relative to the longitudinal axis, the position of the point *O* of the beginning of the connected coordinate system *OXYZ* does not affect the relative movement of the critical jack during the movements of DOF6 along roll;

– when DOF6 yaws, the best position is the position of the point *O* of the beginning of the connected coordinate system *OXYZ* at 1/3 of the height of the DOF6 triangle $K_1K_2K_3$ (Fig. 5), and when DOF6 pitches – at 1/2 the height of the DOF6 triangle $K_1K_2K_3$.

Since pitch movement is more informative for the pilot than yaw movement, the best position of the point *O* of the beginning of the connected *OXYZ* coordinate system for DOF6 movements along individual degrees of freedom is 1/2 the height of the triangle $K_1K_2K_3$ (Fig. 2).

The results of calculations, which are given in Table. 4, show:

– only along the longitudinal degree of freedom, the operating ranges of DOF6 movements are sufficient for motion cueing;

– only DOF6-1.5 has a sufficient working range of DOF6 movements along the lateral degree of freedom, and for DOF6-1 it is necessary to abandon the static motion cues;

– no DOF6 has a sufficient working range of movement along the vertical degree of freedom;

– in order to improve the quality of motion cueing along the lateral degree of freedom, it is necessary to slightly reduce the working range of DOF6 movement along the pitch;

– when changing the direction of the longitudinal axis to the opposite (DOF6-1 (II)), the operating ranges of DOF6 movements along all degrees of freedom, except for the vertical, remain unchanged, and along the vertical – slightly increased.

The results given in Table 5 show that the maximum utilization of DOF6 structural resources significantly expanded its working range of movements:

– vertical movement of DOF6 increased by 29 %,

– lateral movement of DOF6 increased by 28 %,

– longitudinal movement of DOF6 increased by 3 %.

Fig. 5–7 (curves 2) show that:

– active restrictions along vertical and lateral degrees of freedom;

– due to a significant structural resource, DOF6-1.5 pitch axis is shifted to the center of gravity of the aircraft in the entire range of angles. Moreover, in the range of angles of 2 degrees, it practically coincides with the center of gravity of the plane, which significantly brings the perception of movement on the simulator and the plane closer.

Fig. 8 shows that:

– the maximum displacements of jacks changed slightly: the maximum displacements of the 2nd jack increased by 18 %, and the 3rd jack decreased by 19 %;

– the nature of the movements of jacks changed significantly: shelves appeared when the 2nd jack moved, and the directions of its movement changed when the 3rd jack moved.

The leading simulator-building companies CAE Electronics and Thales Training & Simulation use DOF6 with a length of jack rods of 2 m. Our solutions close the problematic part of the optimal utilization of DOF6 structural resources owing to results obtained. First, it is the operator of the movement of jacks depending on the required movements of DOF6 along the degrees of freedom determined by the permissible and maximum working ranges of DOF6 movements. These results made it possible to determine the structural resources of DOF6. Secondly, it is the use of the determined optimal coordinate of the point *O* of the beginning of the connected coordinate system *OXYZ* along the longitudinal axis *OX* and the described coordinates of the centers of the axes of rotation of the motion system by cubic spline functions. Owing to this, it became possible to optimally use the specified design resources of DOF6-1.5 and to use these motion systems as part of flight simulators

to motion cueing (instead of DOF6 with the length of the jack rods of 2 m).

The limitations of this study include the need to control the characteristics of jacks and DOF6 to avoid the appearance of false motion cues. They must be taken into account when trying to apply it in practice, as well as in further theoretical studies.

The disadvantages of the study are the lack of consideration of the real characteristics of jacks and DOF6. Therefore, consideration of such characteristics may be chosen as a possible direction for further research.

7. Conclusions

1. The dependence of the coordinates of the centers of rotation of the upper hinges of jacks in the Earth's coordinate system $O_gX_gY_gZ_g$ has been constructed. The coordinates of the centers of rotation of the lower hinges of jacks in the Earth coordinate system $O_gX_gY_gZ_g$ and the coordinates of the centers of rotation of the upper hinges of jacks in the connected coordinate system $OXYZ$ have been determined. A system of nonlinear equations has been built that fully determines the dependence of the movements of jacks on the movement of DOF6 along individual degrees of freedom.

2. The coordinate of the point O of the beginning of the connected coordinate system $OXYZ$ along the longitudinal axis OX on DOF6 can be chosen arbitrarily. And the stated problem of choosing this point made it possible to select its coordinate that improves the motion cueing on DOF6.

3. Displacement of the coordinates of the pitch and yaw axes along the direction of the center of gravity of the aircraft provides an increase in linear accelerations of DOF6 due to angular movements, i.e., it improves the motion cueing. Reducing the problem to an extreme one makes it possible to determine the permissible displacements of DOF6.

4. Using the known minimum ranges of DOF6 movement along individual degrees of freedom to motion cueing, the problem of determining the maximum working ranges of the movement of DOF6 was stated and solved. The geometric meaning of this problem implies fitting three parallelepipeds one after the other into the area of possible positions of DOF6, namely:

– a parallelepiped, the length of one edge of which is equal to the minimum necessary range of DOF6 movement along the yaw, and the length of the other two edges is not less than the minimum necessary ranges of DOF6 movement along the pitch and longitudinal degrees of freedom;

– a parallelepiped, the length of one edge of which is equal to the minimum necessary range of DOF6 movement along roll, and the length of the other two edges is not less than the minimum necessary ranges of DOF6 movement along the pitch and vertical degrees of freedom;

– a hyper parallelepiped, the lengths of two edges of which are equal to the minimum necessary ranges of DOF6 movement, along roll and yaw, and the lengths of its other two edges are not less than the minimum necessary ranges of DOF6 movement along pitch and lateral degrees of freedom.

5. In order to improve the quality of motion cueing and the efficiency of using the structural resource, the working range of DOF6 pitch movements is divided into subintervals, and the coordinates of the pitch and yaw axes are described by cubic spline functions. On the basis of the discrepancy between the permissible and working range of DOF6 movements, a criterion for evaluating the structural resources of DOF6 was developed based on linear degrees of freedom, taking into account the peculiarities of piloting a non-maneuverable aircraft and the perception of motion cues. We have stated and solved an extreme problem of determining the dependence of the coordinates of the pitch and roll axes along the pitch angle, taking into account the maximum use of the structural resources of DOF6.

Conflicts of interest

The authors declare that they have no conflicts of interest in relation to the current study, including financial, personal, authorship, or any other, that could affect the study and the results reported in this paper.

Funding

The study was conducted without financial support.

Data availability

All data are available in the main text of the manuscript.

References

1. Kabanyachyi, V., Sukhov, V. (2022). Sensor calibration of flight simulator motion system. Modern Engineering and Innovative Technologies, 1 (22-01), 127–134. doi: https://doi.org/10.30890/2567-5273.2022-22-01-021
2. Andrievskiy, B. R., Arseniev, D. G., Zegzhda, S. A., Kazunin, D. V., Kuznetsov, N. V., Leonov, G. A. et al. (2017). Dynamics of the Stewart platform. Vestnik of Saint Petersburg University. Mathematics. Mechanics. Astronomy, 4 (62 (3)), 489–506. doi: https://doi.org/10.21638/11701/spbu01.2017.311
3. Chandrasekaran, K., Theningaledathil, V., Hebbar, A. (2021). Ground based variable stability flight simulator. Aviation, 25 (1), 22–34. doi: https://doi.org/10.3846/aviation.2021.13564
4. Markou, A. A., Elmas, S., Filz, G. H. (2021). Revisiting Stewart-Gough platform applications: A kinematic pavilion. Engineering Structures, 249, 113304. doi: https://doi.org/10.1016/j.engstruct.2021.113304
5. Hurtasenko, A., Chuev, K., Voloshkin, A., Cherednikov, I., Gavrilov, D. (2022). Optimization of the design parameters of robotic mobility platforms for training machine operators on the simulator and the implementation of the required trajectories. Bulletin of Belgorod State Technological University Named after. V. G. Shukhov, 7 (4), 101–115. doi: https://doi.org/10.34031/2071-7318-2021-7-4-101-115

6. Daş, T., Kumpas, I. (2019). Mathematical Modelling, Simulation and Application of Full Flight Helicopter Simulator. Uluslararası Muhendislik Arastirma ve Gelistirme Dergisi, 11 (1), 135–140. doi: https://doi.org/10.29137/umagd.454156
7. Virgil Petrescu, R. V., Aversa, R., Apicella, A., Kozaitis, S., Abu-Lebdeh, T., Petrescu, F. I. T. (2018). Inverse Kinematics of a Stewart Platform. Journal of Mechatronics and Robotics, 2 (1), 45–59. doi: https://doi.org/10.3844/jmrsp.2018.45.59
8. Sapunov, E. A., Proshin, I. A. (2011). Modeling of the dynamic stand drive at aviation training simulator. Yzvestyia Samarskoho nauchnoho tsentra Rossyiskoi akademiy nauk, 13 (1-2), 337–340.
9. Scholten, P. A., van Paassen, M. M., Chu, Q. P., Mulder, M. (2020). Variable Stability In-Flight Simulation System Based on Existing Autopilot Hardware. Journal of Guidance, Control, and Dynamics, 43 (12), 2275–2288. doi: https://doi.org/10.2514/1.g005066
10. Silva, D., Garrido, J., Riveiro, E. (2022). Stewart Platform Motion Control Automation with Industrial Resources to Perform Cycloidal and Oceanic Wave Trajectories. Machines, 10 (8), 711. doi: https://doi.org/10.3390/machines10080711
11. Velasco, J., Calvo, I., Barambones, O., Venegas, P., Napole, C. (2020). Experimental Validation of a Sliding Mode Control for a Stewart Platform Used in Aerospace Inspection Applications. Mathematics, 8 (11), 2051. doi: https://doi.org/10.3390/math8112051
12. Yang, F., Tan, X., Wang, Z., Lu, Z., He, T. (2022). A Geometric Approach for Real-Time Forward Kinematics of the General Stewart Platform. Sensors, 22 (13), 4829. doi: https://doi.org/10.3390/s22134829
13. Teodorescu, P. P. (2007). Kinematics. Mathematical and Analytical Techniques with Applications to Engineering, 287–351. doi: https://doi.org/10.1007/1-4020-5442-4_5